HETEROCYCLES, Vol. 103, No. 2, 2021, pp. 893 - 901. © 2021 The Japan Institute of Heterocyclic Chemistry
Received, 30th November, 2020, Accepted, 8th March, 2021, Published online, 18th March, 2021
DOI: 10.3987/COM-20-S(K)55

STEREOSELECTIVITY OF THE BIGINELLI REACTION CATALYZED BY CHIRAL PRIMARY AMINE: A COMPUTATIONAL STUDY

Takayoshi Yoshimura,[1‡] Maneeporn Puripat,[1‡] Vudhichai Parasuk,[2] and Miho Hatanaka[1,3]*

[1]Department of Chemistry, Faculty of Science and Technology, Keio University, 3-14-1 Hiyoshi, Kohoku-ku, Yokohama, Kanagawa 223-8522, Japan; [2]Department of Chemistry, Faculty of Science, Nanoscience and Technology Program, Graduate School, Chulalongkorn University, 254 Phayathai Road, Pathumwan, Bangkok 10330, Thailand; [3]Division of Materials Science, Graduate School of Science and Technology, Nara Institute of Science and Technology, 8916-5 Takayama-cho, Ikokma, Nara 630-0192, Japan. ‡Contributed equally to this work; E-mail : hatanaka@chem.keio.ac.jp

Abstract – The Biginelli reaction catalyzed by a chiral compound is one of the most effective ways to form bioactive heterocycle compounds. High enantioselectivity was obtained using primary amine with a chiral diamine backbone as a chiral catalyst. To elucidate the origin of the enantioselectivity, we investigated the reaction pathways of this catalytic reaction using the density functional theory. We also focused on the transition states of the rate-determining step leading different stereoisomers. The rate-determining step was the proton transfer process accompanying the cyclization of the substrate, which was mediated by the amide moiety of the catalyst, and the orientation of the amide moiety was the reason for the enantioselectivity.

INTRODUCTION

3,4-Dihydropyrimidin-2(1*H*)-ones (or -thiones), referred to as DHPMs, have attracted significant attention as bioactive compounds. It is known to have versatile biological activity and can be used as calcium channel modulators, mitotic kinesin inhibitors, adrenergic receptor antagonists, and anti-bacterial, antiviral, and anticancer drugs.[1] DHPMs have a chiral center and their enantiomers have been found to exhibit different pharmaceutical activities. Thus, efficient synthesis of optically pure DHPMs is in great demand. One of the effective ways to form DHPMs is the Biginelli reaction, which is a three component

one-pot reaction involving aldehyde, (thio)urea, and β–keto ester.[2-5] Enantioselective Biginelli reactions have been carried out by a number of chiral metal complex catalysts,[6,7] and chiral organocatalysts, such as primary amines,[8,9] proline derivatives,[10-12] pyrrolidinyl tetrazoles,[13] pyrazolidine,[14] quinidine-based thiourea,[15] phosphoric acids,[16,17] bisphosphorylimide,[18] and nanocomposites.[19] Among them, primary amine with a chiral diamine backbone is one of the most efficient chiral catalysts. Scheme 1a shows the Biginelli reaction of benzaldehyde **1**, urea **2**, and ethyl acetoacetate **3** catalyzed by a primary amine with (1*R*,2*R*)-cyclohexane-1,2-diamine backbone **5**.[8] The DHPM derivative **4** with *R*-configuration was obtained with excellent enantioselectivity up to > 99% ee under the room temperature. High enantioselectivities were also achieved in other non-polar solvents, while the enantioselectivity reduced in polar solvents, such as water, ethanol, and DMSO.

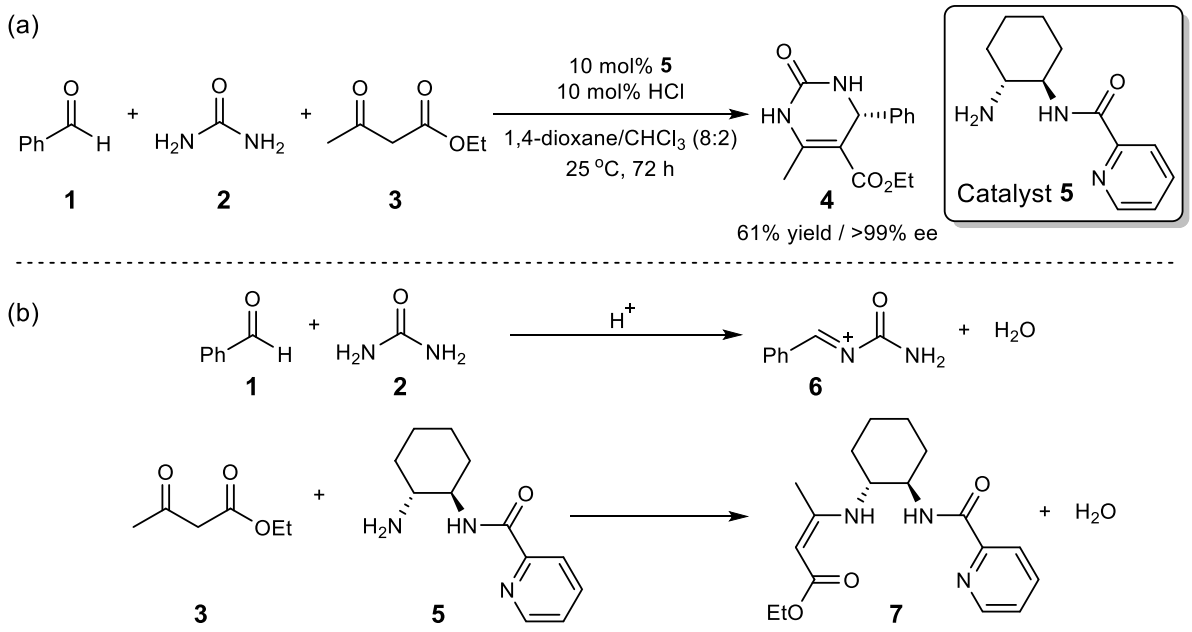

Scheme 1. Biginelli reaction catalyzed by the chiral primary amine[8] (a) and its possible early-stage reactions (b)

Computational studies are necessary to obtain a comprehensive understanding of this mechanism. We previously reported the density functional theory (DFT) study on the Biginelli reaction involving same reagents **1**, **2**, and **3** (without any chiral catalyst) and clarified three new insights on the mechanism.[20] First, the reaction started with the condensation of benzaldehyde **1** and urea **2**, leading to the iminium intermediate **6** (see Scheme 1b), followed by the addition of ethyl acetoacetate **3**. This mechanism is known as the "iminium route". Second, the excess amount of urea **2** played the role of a catalyst to accelerate the reaction between iminium intermediate **6** and ethyl acetoacetate **3**. Third, the rate-determining step was the cyclization step *via* the C-N bond formation between iminium intermediate

6 and ethyl acetoacetate **3**. Comparing the reactions with and without the chiral catalyst **5**, the early stage of the reaction pathway could be the same. In other words, the iminium intermediate **6** could be formed from **1** and **2**, which was supported by the experimental fact that the iminium intermediate **6** and ethyl acetoacetate **3** afforded (*R*)-**4** in 98% ee using the catalyst **5**.[8] In addition, the amine moiety of **5** could activate acetoacetate **3** and form enamine intermediate **7** (see Scheme 1b) as proposed in secondly amine catalyzed Biginelli reactions.[6,10-14] Thus, to elucidate the origin of the enantioselectivity, we investigate the reaction pathways based on the DFT method, focusing on the reaction between iminium **6** and enamine **7**, especially the transition states (TSs) of the rate-determining step.

RESULTS AND DISCUSSION

First, we focus on the structure of the enamine intermediate **7**, activated **3** by the amine catalyst **5**. The conformers of **7** were explored using an automated reaction path search method called the anharmonic downward distortion following (ADDF) method.[21] Figure 1 shows four conformers of **7**. In the case of the most stable conformer **7a**, the *si*-face of the enamine carbon (highlighted in pink in Figure 1) faced the picolinamide moiety. The *si*-face of the enamine carbon was also covered by the picolinamide moiety in other conformers **7b**-**7h**, whose Gibbs free energy differences from **7a** were less than 3.0 kcal mol^{-1} (see Figure S1).

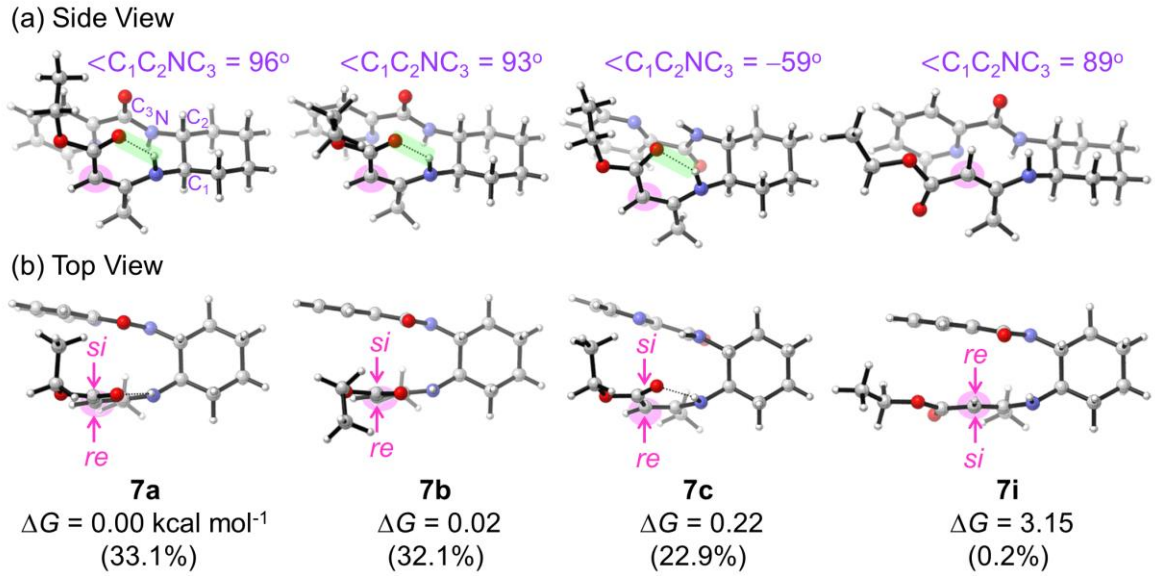

Figure 1. Side (a) and top views (b) of the four conformers of the enamine intermediate **7**. Other stable conformers are shown in Figure S1. The geometries were optimized at the B3LYP-D3/6-31G(d,p) level with the PCM (1,4-dioxane). The Gibbs free energy differences ΔG (in kcal mol^{-1}) relative to **7a** were computed using the Gibbs free energy correction under 298.15 K and 1 atm and the single point energy at B3LYP-D3/6-311G(3df,3pd) with the PCM level of theory. The existing probabilities (in %) were shown in parentheses.

Their structural differences observed from **7a** were only the orientations of the ethyl group and/or amide moiety. Among them, the existing probabilities of the three most stable conformers **7a**, **7b**, and **7c** were higher than 20%, which indicated that the ethyl group and the amide moiety (see their CCNC dihedral angles in Figure 1) could rotate easily. The conformers, in which the *re*-face of the enamine carbon faced the picolinamide moiety were also found (such as **7i**). However, they were less stable than **7a** by at least 3.1 kcal mol^{-1} because the hydrogen bond between the hydrogen of the enamine moiety and one of the oxygen atoms of the ester moiety (highlighted in green in Figure 1) was dissociated due to the rotation of the enamine moiety.

Second, the C-C bond formation between **6** and **7**, which afforded intermediate **8**, was investigated. The intermediate **8** has two chiral C atoms on the enamine moiety and the iminium moiety as highlighted in pink and yellow, respectively, in Figure 2a. The chirality on the enamine moiety and the iminium moiety can be determined by the approach direction of **6** and the molecular plane of **7**. Thus, we named the reaction pathways of four different configurations (*re*,*re*), (*re*,*si*), (*si*,*re*) and (*si*,*si*)-pathways as shown in Figure S2. Even though **8** has two chiral centers, the final product **4** has only one chiral center (in yellow) because the sp^3 carbon on the ethyl acetate moiety (in pink) become the sp^2 carbon due to the dehydration at the final stage of the reaction. Therefore, the (*si*,*si*)- and (*si*,*re*)-pathways lead to the (*R*)-**4** product, and the (*re*,*re*)- and (*re*,*si*)-pathways lead to the (*S*)-**4** product.

Focusing on the stable conformers of **7a-7h**, the *si*-face attack of **6** to **7a-7h** seemed to be blocked by picolinamide moiety. However, the Gibbs free energies of the TSs of the C-C bond formation *via* the *si*- and *re*-face attacks were similar, as shown in Figure 2a. As highlighted in green in Figure 2b, the iminium moiety was activated *via* the hydrogen bond from the oxygen atom of the picolinamide moiety of **7**. To form this hydrogen bond, **6** was needed to be inserted between the picolinamide moiety and the enamine moiety of **7**, which induced the rotation of the enamine moiety, resulting in both *si*- and *re*-faces of enamine moiety being open. The intermediate **8** was only 1–3 kcal mol^{-1} more stable than the pre-reaction complex **6…7**, and the activation barrier of the C-C bond formation was less than 5 kcal mol^{-1}. Thus, both the forward and backward reactions took place rapidly, *i.e.* **6…7** and **8** were in equilibrium. Therefore, the stereoselectivity could be determined after the C-C bond formation step, *i.e.* the cyclization step.

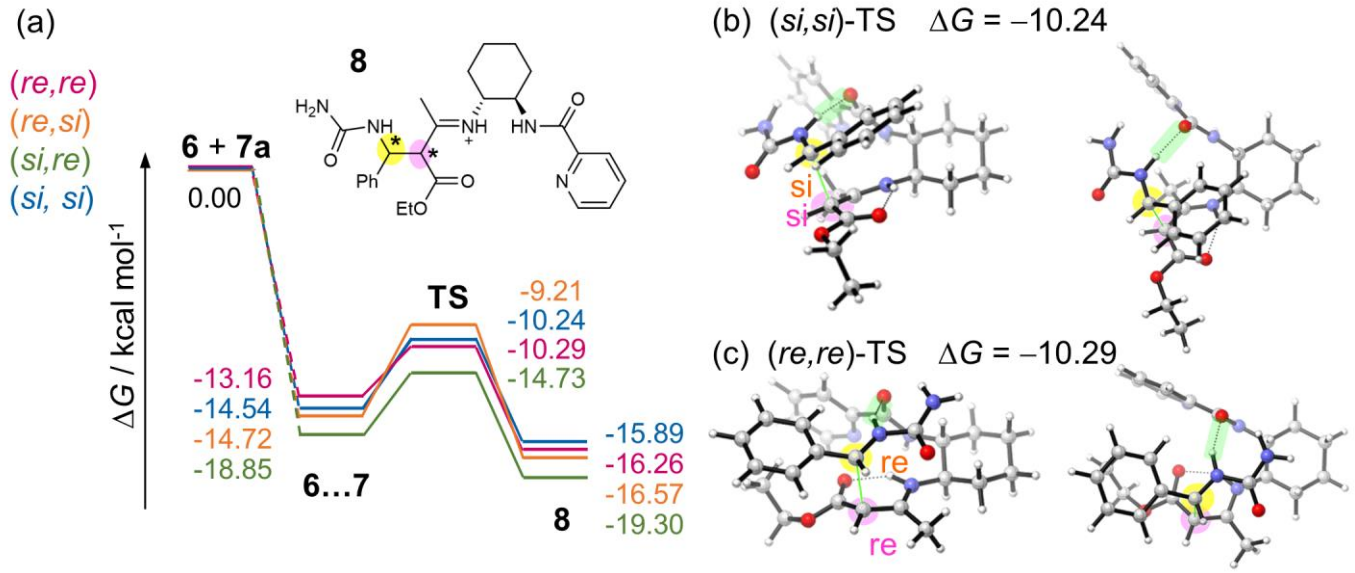

Figure 2. The Gibbs free energy profile Δ*G* (in kcal mol^{-1}) of the C-C bond formation step between **6** and **7** (a) and the geometries of the (*si*,*si*)-TS (b) and (*re*,*re*)-TS (c). The geometries were optimized at the B3LYP-D3/6-31G(d,p) level with the PCM (1,4-dioxane). The Gibbs free energy differences Δ*G* (in kcal mol^{-1}) relative to the dissociation limit of **6** and **7a** were computed using the Gibbs free energy correction under 298.15 K and 1 atm, and the single point energy at B3LYP-D3/6-311G(3df,3pd) with the PCM level of theory.

Next, the cyclization step following the C-C bond formation was focused on. As shown in Figure 3, the cyclization involved three steps: C-N bond formation followed by the proton transfer from the N atom of the iminium moiety to the N atom of the cyclohexane-diamine moiety through the O atom of the picolinamide moiety. These steps took place step-by-step, even for the reaction through the (*re*,*re*)-TS (see the IRC path on Figure S3). The first step of the cyclization, C-N bond formation, involved the conformation change from **8** to **8'**. The (*re, si*)-**8'** and (*si, re*)-**8'** were more than 10 kcal mol^{-1} higher than the (*re, re*)-**8'** and (*si, si*)-**8'**. Even though the stability of **8'** depended on the configurations, the enantio excess could be determined by the Gibbs free energy difference between the most stable intermediate **8** and the TS of the rate-determining step. Considering the Boltzmann distribution of the TSs of the rate-determining step, we estimated that the major product had (*R*)-configuration and the enantio excess was 91% ee, which was consistent with the experimental fact ((*R*)-product, 99% ee).[8] Note that we also computed the TSs of the cyclization, in which the picolinamide O atom did not mediate the proton transfer (see Figure S4) and an additional water molecule mediated the proton transfer (see Figure S5). Their Gibbs free energies were more than 4 kcal mol^{-1} higher than the rate-determining TSs shown in Figure 3. Thus, it can be said that the picolinamide O atom had a critical role to accelerate the proton transfer.

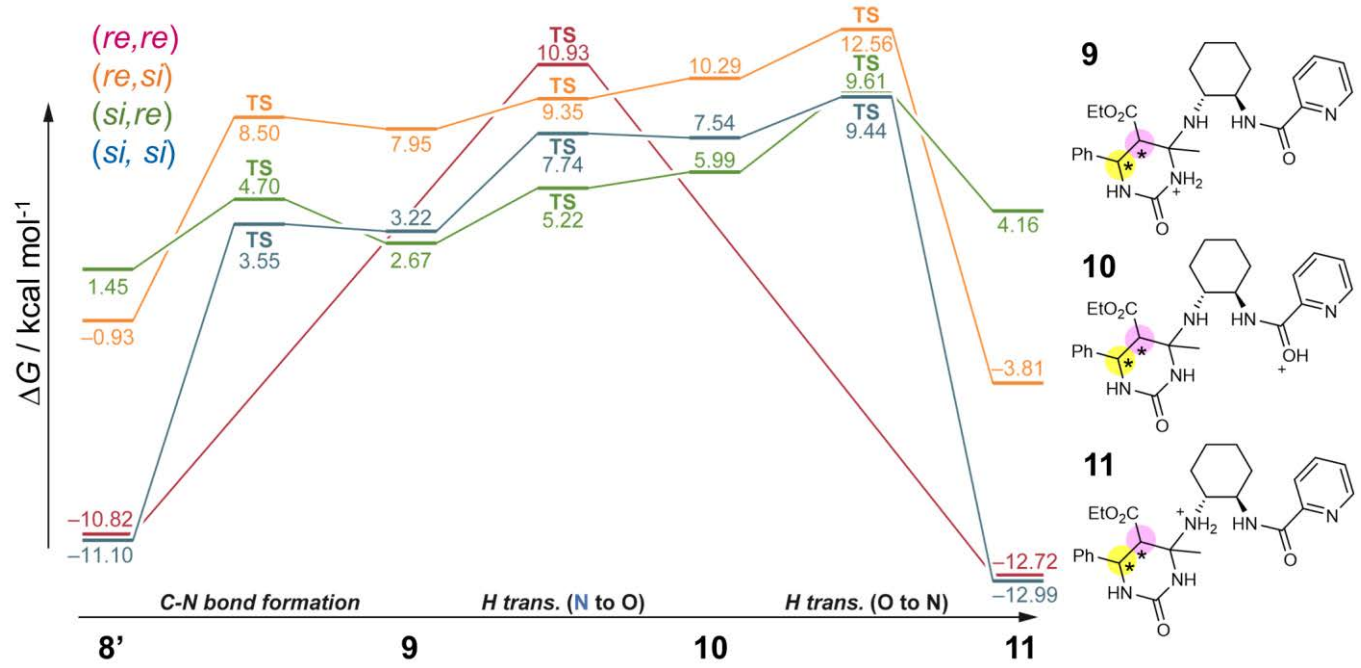

Figure 3. The Gibbs free energy profile Δ*G* (in kcal mol^{-1}) of the cyclization step starting from the intermediate **8'**. The reference of the Gibbs free energy profile (Δ*G* = 0.0) was the dissociation limit of **6** and **7a**. The geometries were optimized at the B3LYP-D3/6-31G(d,p) level with the PCM (1,4-dioxane). The Gibbs free energy corrections were computed under 298.15 K and 1 atm condition, and the single point calculations were carried out at B3LYP-D3/6-311G(3df,3pd) with the PCM level of theory.

Finally, to understand the origin of the enantioselectivity, the geometries of the TSs of the rate-determining step were compared. As mentioned above, the proton transfer from the N atom of the iminium moiety to the N atom of the cyclohexane-diamine moiety was mediated by the O atom of the picolinamide moiety. At the same time, the N atom on the diamine moiety formed a hydrogen bond with the O atom of the ethyl acetate moiety. Thus, the distances related to the hydrogen bond network could be the key to determine the energy differences. Focusing on the distance between the H on the diamine moiety and the O on the ethyl acetate moiety, the TS energy level lowered with decreasing the O-H distance. As highlighted in red in Figure 4, the O-H distance was the shortest (1.93 Å) in the most stable (*si*,*si*)-TS and the longest (2.73 Å) in the most unstable (*re*,*si*)-TS. The shorter O-H bond resulted in the higher nucleophilicity of the diamine N and the stronger hydrogen bond between the diamine N atom (proton acceptor) and the picolinamide O atom (proton transfer mediator) (shown in green line in Figure 4). Actually, this N-O distance tended to be shorter in the stable TSs ((*si*,*si*) and (*si*,*re*)), which afforded the major stereoisomer (*R*)-**4**. Therefore, the energy difference between the TSs leading (*R*)- and (*S*)-**4** mainly came from the different intramolecular hydrogen bond network distances.

The effect of the intramolecular hydrogen bond on the enantioselectivity could be one of the reasons of the enantio excess dependency on the solvent. As mentioned in the introduction, enantiomeric excess was reduced in polar solvents such as water, ethanol, and DMSO.[8] These three solvent molecules were proton acceptors, *i.e.* proton transfer mediators. Thus, the proton transfer for (*re,re*)- and (*re,si*)-structures might be accelerated by the solvent molecules, which caused the increase of the production of the minor stereo-isomer (*S*). In summary, the small difference of the intramolecular hydrogen bond network involving the O atom of the picolinamide moiety caused the enantioselectivity. Though amide moiety and cyclohexyl-diamine moieties could not be modified because they were critical for the hydrogen bond network structure, the phenyl groups on the aldehyde **1** were relatively far from the hydrogen bond network center. Therefore, this catalytic system might be applicable to a wide range of aldehydes.

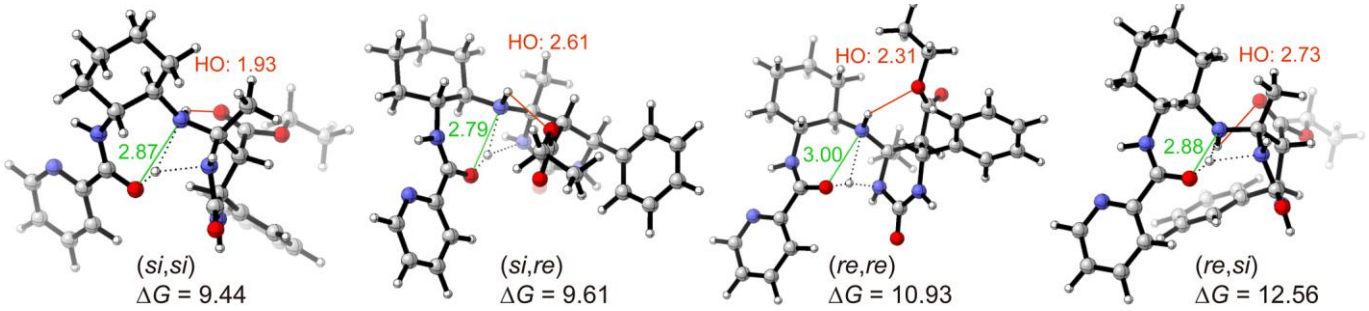

Figure 4. The geometries of the transition states of the rate-determining step for four stereoisomers, (*si*,*si*), (*si, re*), (*re, re*), and (*re*,*si*). The Gibbs free energy differences Δ*G* are in kcal mol^{-1}. The reference of the energies (Δ*G* = 0.0) was the dissociation limit of **6** and **7a**. The geometries were optimized at the B3LYP-D3/6-31G(d,p) level with the PCM (1,4-dioxane). The Gibbs free energy corrections were computed under 298.15 K and 1 atm condition, and the single point energy at B3LYP-D3/6-311G(3df,3pd) with the PCM level of theory.

COMPUTATIONAL

First, the conformers of the intermediate **7** obtained by the condensation of catalyst **5** and ethyl acetoacetate **3** were explored using the ADDF method,[21] in which the potential energy surface was computed with the semi-empirical PM6 level of theory.[22] Then, all the conformers were reoptimized at the DFT method. The geometry optimizations as well as frequency calculations were performed at the dispersion corrected[23] B3LYP-D3/6-31G(d,p) level.[24-26] The electronic energies were refined by the single-point calculations at the B3LYP-D3/6-311G(3df,3pd) level.[27] The Gibbs free energy corrections were computed at 1 atm and 298.15 K. In all calculations, the solvation effect was included by the polarized continuum model (PCM)[28] using the dielectric constant of 2.2099 for 1,4-dioxane. Some of the TSs were explored using the artificial force induced reaction (AFIR) method, which is one of the

automated reaction path search methods.[29,30] All the transition states were confirmed by the intrinsic reaction coordinate (IRC) calculations.[31] All the optimizations, frequency calculations, IRC calculations were performed using the Global Reaction Route Mapping (GRRM) program[32] using energies and energy derivatives computed with the Gaussian 09 program.[33]

ACKNOWLEDGEMENTS

This work was supported by JSPS KAKENHI Grant no. JP17H06445, 18H03908, and 20K05438. We also acknowledge the computer resources provided by the Academic Center for Computing and Media Studies (ACCMS) at the Kyoto University and by the Research Center of Computer Science (RCCS) at the Institute for Molecular Science.

REFERENCES AND NOTES

1. A. Dömling, W. Wang, and K. Wang, *Chem. Rev.*, 2012, **112**, 3083.
2. H. G. O. Alvim, T. B. Lima, A. L. de Oliveira, H. C. B. de Oliveira, F. M. Silva, F. C. Gozzo, R. Y. Souza, W. A. da Silva, and B. A. D. Neto, *J. Org. Chem.*, 2014, **79**, 3383.
3. E. Marcantoni and M. Petrini, *Adv. Synth. Catal.*, 2016, **358**, 3657.
4. H. Nagarajaiah, A. Mukhopadhyay, and J. N. Moorthy, *Tetrahed Lett.*, 2016, **57**, 5135.
5. M. Oliverio, P. Costanzo, M. Nardi, I. Rivalta, and A. Procopio, *ACS Sustain. Chem. Eng.*, 2014, **2**, 1228.
6. Y. Huang, F. Yang, and C. Zhu, *J. Am. Chem. Soc.*, 2005, **127**, 16386.
7. P. Karthikeyan, S. A. Aswar, P. N. Muskawar, P. R. Bhagat, and S. S. J. Kumar, *J. Organomet. Chem.*, 2013, **723**, 154.
8. D. Z. Xu, H. Li, and Y. M. Wang, *Tetrahedron*, 2012, **68**, 7867.
9. Y. Y. Wang, J. Yu, Z. Miao, and R. Chena, *Adv. Synth. Catal.*, 2009, 351, 3057.
10. J. Xin, L. Chang, Z. Hou, D. Shang, X. Liu, and X. Feng, *Chem. Eur. J*, 2008, **14**, 3177.
11. J. H. C. Sohn, H. M. Lee, S. Joung, and S. H. Y. Lee, *Eur. J. Org. Chem.*, 2009, 3858.
12. S. Saha and J. N. Moorthy, *J. Org. Chem.*, 2011, **76**, 396.
13. Y. Y. Wu, Z. Chai, X. Y. Liu, G. Zhao, and S. W. Wang, *Eur. J. Org. Chem.*, 2009, 904.
14. X. H. Chen, X. Y. Xu, H. Liu, L. F. Cun, and L. Z. Gong, *J. Am. Chem. Soc.*, 2006, **128**, 14802.
15. Z. Hang, J. Zhu, X. Lian, P. Xu, H. Yu, and S. Han, *Chem. Commun.*, 2016, **52**, 80.
16. I. Suzuki, Y. Iwata, and K. Takeda, *Tetrahedron Lett.*, 2008, **49**, 3238.
17. N. Li, X. H. Chen, J. Song, S. W. Luo, W. Fan, and L. Z. Gong, *J. Am. Chem. Soc.*, 2009, **131**, 15301.
18. D. An, Y. S. Fan, Y. Gao, Z. Q. Zhu, L. Y. Zheng, and S. Q. Zhang, *Eur. J. Org. Chem.*, 2014, 301.

19. Y. Titova, O. Fedorova, G. Rusinov, A. Vigorov, V. Krasnov, A. Murashkevich, and V. Charushin, *Catal. Today*, 2015, **241**, 270.
20. M. Puripat, R. Ramozzi, M. Hatanaka, W. Parasuk, V. Parasuk, and K. Morokuma, *J. Org. Chem.*, 2015, **80**, 6959.
21. S. Maeda, T. Taketsugu, K. Morokuma, and K. Ohno, *Bull. Chem. Soc. Jpn.*, 2014, **87**, 1315.
22. J. J. P. Stewart, *J. Mol. Model.*, 2007, **13**, 1173.
23. S. Grimme, J. Antony, S. Ehrlich, and H. Krieg, *J. Chem. Phys.*, 2010, **132**, 154104.
24. A. D. Becke, *Phys. Rev. A*, 1988, **38**, 3098.
25. C. Lee, W. Yang, and R. G. Parr, *Phys. Rev. B*, 1988, **37**, 785.
26. G. A. Petersson, A. Bennett, T. G. Tensfeldt, M. A. Al-Laham, W. A. Shirley, and J. Mantzaris, *J. Chem. Phys.*, 1988, **89**, 2193.
27. A. D. McLean and G. S. Chandler, *J. Chem. Phys.*, 1980, **72**, 5639.
28. J. Tomasi, B. Mennucci, and R. Cammi, *Chem. Rev.*, 2005, **105**, 2999.
29. S. Maeda, K. Ohno, and K. Morokuma, *Phys. Chem. Chem. Phys.*, 2013, **15**, 3683.
30. S. Maeda, Y. Harabuchi, M. Takagi, K. Saita, K. Suzuki, T. Ichino, Y. Sumiya, K. Sugiyama, and Y. Ono, *J. Comput. Chem.*, 2018, **39**, 233.
31. K. Fukui, *Acc. Chem. Res.*, 1981, **14**, 363.
32. GRRM17: S. Maeda, Y. Osada, T. Taketsugu, K. Morokuma, and K. Ohno, http://iqce.jp/GRRM/index_e.shtml.
33. Gaussian 09, Revision E.01, M. J. Frisch, G. W. Trucks, H. B. Schlegel, G. E. Scuseria, M. A. Robb, J. R. Cheeseman, G. Scalmani, V. Barone, B. Mennucci, G. A. Petersson, H. Nakatsuji, M. Caricato, X. Li, H. P. Hratchian, A. F. Izmaylov, J. Bloino, G. Zheng, J. L. Sonnenberg, M. Hada, M. Ehara, K. Toyota, R. Fukuda, J. Hasegawa, M. Ishida, T. Nakajima, Y. Honda, O. Kitao, H. Nakai, T. Vreven, J. A. Montgomery, Jr., J. E. Peralta, F. Ogliaro, M. Bearpark, J. J. Heyd, E. Brothers, K. N. Kudin, V. N. Staroverov, T. Keith, R. Kobayashi, J. Normand, K. Raghavachari, A. Rendell, J. C. Burant, S. S. Iyengar, J. Tomasi, M. Cossi, N. Rega, J. M. Millam, M. Klene, J. E. Knox, J. B. Cross, V. Bakken, C. Adamo, J. Jaramillo, R. Gomperts, R. E. Stratmann, O. Yazyev, A. J. Austin, R. Cammi, C. Pomelli, J. W. Ochterski, R. L. Martin, K. Morokuma, V. G. Zakrzewski, G. A. Voth, P. Salvador, J. J. Dannenberg, S. Dapprich, A. D. Daniels, O. Farkas, J. B. Foresman, J. V. Ortiz, J. Cioslowski, D. J. Fox, Gaussian, Inc., Wallingford CT, 2010.